J Mater Sci (2006) 41:4937–4943
DOI 10.1007/s10853-006-0320-4

Textured mullite at muscovite–kaolinite interface

G. Lecomte · P. Blanchart

Received: 27 July 2004 / Accepted: 15 September 2005 / Published online: 27 May 2006

Abstract Mullite crystallization was carried out by the inter-reaction of alternate layers of muscovite and kaolinite minerals. The nucleation and growth of mullite anisotropic crystals take place along the muscovite plane and specific structural relationships are observed, which confirm a topotactic effect with the high temperature form of muscovite. The $[001]_{mull}$ axis is oriented parallel to $[010]_{musc}$, $[310]_{musc}$ and $[\bar{3}10]_{musc}$ axes. The mullite orientation is fully completed in a temperature range between the ternary eutectic at 985 °C and the ternary transition point at 1140 °C, of the SiO_2–Al_2O_3–K_2O system, which strongly suggests an influence of a small quantity of liquid phase at the interface. Along the kaolinite–muscovite interface, the realisation of highly textured ceramics can be achieved.

Introduction

Properties of ceramic materials can be improved by the spatial organization of their microstructure. Textured ceramics are promising materials for numerous applications in fields of electrical [1]–[3] or mechanical properties [4]. One way to the development of texture is the in-situ formation of anisotropic grains, most often by a template technique. The regulation of orientation can be performed by seed particles [5] or by epitaxy on various substrates [6, 7]. In this study, we used large flakes of muscovite mica as substrates for templating the mullite growth.

G. Lecomte · P. Blanchart (✉)
GEMH, ENSCI, Limoges, France
e-mail: p_blanchart@ensci.fr

Minerals of the mica group, including muscovite, are 2:1 layer silicates formed from a sandwich of two tetrahedral layers—sheets of linked $[SiO_4]$ tetrahedra—joined by a layer of Al^{3+} in octahedral coordination. This octahedral layer is a gibbsite-like structure, with some coordinations by OH groups. Interlayer cations (K^+) compensate the overall negative charge due to various cation substitutions.

A typical reaction during thermal transformation of muscovite is the progressive dehydroxylation in a wide temperature interval, 800–1100 °C with a very broad endothermic reaction [8]. But well crystallized muscovite and large crystals retain OH groups more effectively, up to 1100 °C [9].

Structural data for dehydroxylated muscovite were obtained by X-ray diffraction studies, up to 700 °C. They all show the existence of a high temperature phase with large distortion in the octahedral layers, the change of Al coordination from 6 to 4 or 5-fold and leads to the rearrangement of the adjacent tetrahedral layers. The cell volume of the high temperature phase increases, which is mainly due to a larger *c* parameter [10, 11] (from 20.0–20.1 Å to 20.2–20.3 Å, depending on authors). Structural models of these phases were assessed recently by high temperature X-ray diffraction (up to 1000 °C) and by thermal analyses [12]. They all show that the formation of the high temperature phase involves the mono-dimensional diffusion mechanism of OH groups or condensed water molecules out of the unit layer.

Muscovite above 1000 °C is strongly dehydroxylated and X-ray reflexion intensities decrease, or vanishes at about 1100 °C [12]. Just below this critical temperature, newly crystallized phases are formed as spinel and mullite and a liquid appears in the 985–1140 °C temperature range, in accordance with the SiO_2–Al_2O_3–K_2O ternary phase diagram [13]. In heterogeneous material at the grain size

scale, the liquid quantity and composition depend on the local chemical composition [14]. Liquid triggers the recrystallization processes since the distribution of species are highly favoured.

In this study we considered the 985–1140 °C temperature range because muscovite structural organization is sufficiently weakened at the atomic scale, which favours atom mobility. Atoms become available for nucleation and growth of new phases such as mullite. Large muscovite flakes retain their layer arrangement up to 1100 °C, but above 1140 °C the liquid phase quantity increases significantly to disorganize the material.

For kaolinite, thermal transformations differ from these of muscovite in both the temperature and the sequence of transformations. Dehydroxylation occurs early, between 500 °C and 650 °C to give a poorly ordered dehydroxylated phase (metakaolinite), which reorganises progressively above 960 °C. This transformation sequence [15, 16] is often affected by disorders in cells at the atomic scale and in the layer stacking [17, 18] Structural models for metakaolinite were proposed from X-rays or NMR techniques [19–21] They all report that Si atoms are maintained in a tetrahedral layers whereas Al coordination varies from 4 or 5 and 6 in a highly disordered layer.

In this study, kaolinite was deposited at the surface of muscovite flakes to form a layered composite material. During heating at 1000–1100 °C, mullite is preferentially crystallized at the interface between metakaolinite particles and mica flakes, which maintain a remaining structural organization. In this temperature range, it is proposed to use the high temperature form of mica as a specific substrate.

Experimental

Two-layer composites were realized with large muscovite flakes (~5 mm) covered by a thick deposit of kaolinite from an aqueous suspension. Kaolinite–muscovite mass ratio was maintained close to 1. Muscovite flakes are from Bihar (India) [22] and kaolinite is the Kg1 [23]. The chemical and mineralogical compositions of these minerals are very close to ideal compositions of kaolinite and muscovite (Table 1). By X-ray diffraction, structural characteristics were found to be very similar to tabulated data in JCPDS files. These results ensure that thermal behaviours of the used minerals will be very similar to those of ideal mineral phases. Composite samples were heated at 1000–1100 °C under air. For SEM observations, the metakaolinite layer was removed by a smooth fluoric acid treatment, to observe the crystallized phases at the muscovite surface.

Structural information was obtained from the diffuse scattering contained in X-ray diffraction data, because heat treated materials are structurally low ordered. The Fourier transformation into real-space coordinates gives the atomic pair distribution function (PDF). The PDF has peaks at characteristic distances separating pairs of atoms and thus it reflects the material structure. The PDF is the sine Fourier transformation of the total scattering structure function, $S(Q)$, where Q is the magnitude of the scattering vector. $S(Q)$ includes both Bragg peaks and the diffuse components of the diffraction spectrum [24]. Thus PDF reflects both the local and average atomic structure of the material. It is sensitive to atomic short range ordering and therefore, suitable in characterizing materials where deviations from the average structure are present.

Data sets were taken from a diffractometer using a conventional X-ray tube as source in symmetrical reflexion geometry (Brüker AXS D5000). The incident beam was selected by a quartz single crystal (1011), to obtain the MoKα radiation (λ = 0.70926 Å). With MoKα radiation, a value of Q_{max} = 16 Å^{-1} was reached.

All corrections were made to the raw data to account for experimental effects such as detector characteristics, background, sample absorption and multiple scattering, to obtain the normalized scattering structure function $S(Q)$. These procedures have already been described [24] and calculations including necessary corrections used the software PDFGetX [25]. This method performs calculations of atom positions without the constraints posed by space group symmetries. Experimental PDF spectrums were fitted with data from an average model of muscovite

Table 1 Compositions of minerals (mass %)

	Kaolin Kg1		Bihar muscovite	
	Chemical	Mineralogical	Chemical	Mineralogical
SiO_2	44.5		45.40	Muscovite ≈ 99
Al_2O_3	39.9	Kaolinite ≈ 96	37.1	
Fe_2O_3	0.20		1.10	
TiO_2	1.4	Quartz < 1	–	
MgO	0.03		0.2	
Na_2O	0.01	Anatase ≈ 1.6	0.18	
K_2O	0.05		11.8	
P_2O_5	0.03	Gibbsite ≈ 1.4	–	
Loss (1000 °C)	13.9		4.3	

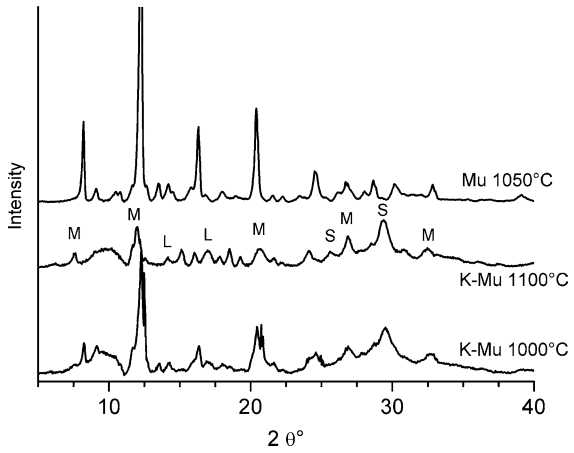

Fig. 1 X-ray (Mo Kα) diffraction of muscovite at 1050 °C. M: mullite; S: spinel; L: leucite

structure, using the profile fitting least-squares regression program PDFFIT [26].

Results

The diffraction pattern of muscovite at 1050 °C has only a few significant reflexions (Fig. 1) and more information was obtained with the experimental PDF (Fig. 2). The maxima of PDF profiles provide information about the bond length distribution between all pairs of atoms within the material. In Fig. 2, the experimental curve is compared with a calculated one using the structural model of 2M1 muscovite [27], in the C2/c space group. Some discrepancies were observed between experimental and calculated PDF. Whereas at short atomic distances only peak positions and amplitudes vary slightly, some significant changes are observed at larger distances. Particularly, peaks from 2M1 muscovite vanished in ranges between 3.8–3.9 Å and 6.8–6.9 Å but new peaks appeared in 4.3–4.4 Å, 5.9–6 Å and 7.4–7.6 Å ranges.

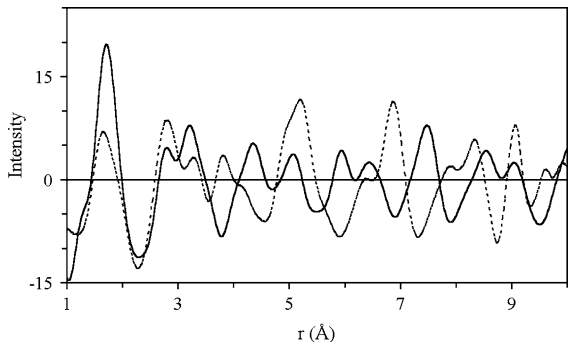

Fig. 2 Experimental PDF of muscovite at 1050 °C (continuous line) and calculated from 2M1 structural model (dashed line)

The calculated PDF contains contributions of all atom pairs and the determination of which atom pair contributes to which peak in the PDF is not always simple with complex structures such as muscovite. Therefore, it might be necessary to calculate a partial PDF related to selected atom pairs. In Fig. 3a, partial PDF of K–Si and K–Al atom contributions shows the decrease of contribution for K–Si distances at 3.78–3.81 Å and for K–Al distances at 5.27–5.30 Å and 6.83–6.70 Å. These distances correspond to interlayer K bonds with neighbouring Si and Al atoms in the muscovite layer. This cast some doubt upon K positions in the high temperature muscovite. For the Si–Al contribution, the comparison of curves in Fig. 3b mainly shows the change of peak positions at long distance ranges (5.26–5.33 Å and 6.7–6.9 Å). It means there are large modifications of the respective structural organization between the outer silica and the inner alumina layer of muscovite.

The PDF refinement of Fig. 2 was carried out with a Si–O distance constrained to known average distances and starting thermal factors from [12]. Although the large number of atom positions, the obtained fit is satisfactory (Fig. 4). The resulting structural arrangement, plotted in Fig. 5 presents similarities with the structural arrangement of high temperature muscovites [10–12], measured at temperatures between 400 °C and 700 °C.

The common features of these published structures are the larger cell volume of the dehydroxylated phase, with respect to the room temperature phase, mainly due to the

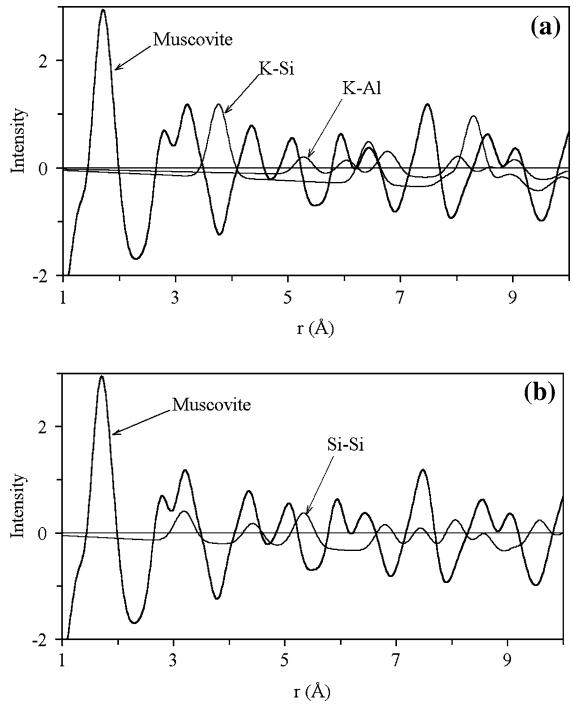

Fig. 3 (**a**): Partial PDF for K–Si and K–Al atom pairs, compared to muscovite PDF at 1050 °C; (**b**): Si-Al contribution to PDF and muscovite PDF at 1050 °C

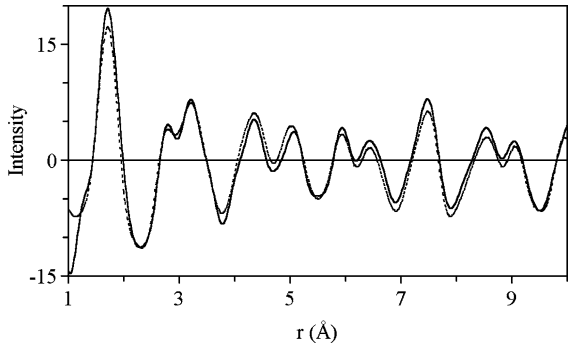

Fig. 4 Experimental (continuous line) and refined PDF (dashed line) for muscovite at 1050 °C

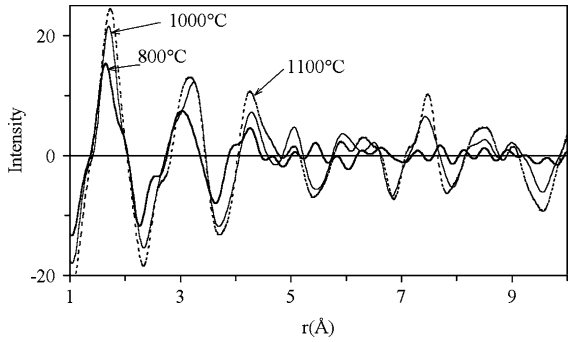

Fig. 6 PDF plots of muscovite–kaolinite composites at 800, 1000 and 1100 °C

increase of the *c* axis [10, 28–31] Besides, some Al atoms switch from 6 to 5 coordination and have a very short bonding distance (down to 1.69 Å) to the oxygen atom shared by two Al atoms [10]. In general, the change of the Al coordination from 6-fold to 5-fold produces an array of oxygen atoms with different charges that triggers the distortion of the adjacent tetrahedral layer. Rotation of tetrahedrons is necessary to compensate the misfit with the distorted octahedral layer.

Correspondingly, our 1050 °C muscovite presents similar transformations (Fig. 5). The unit cell dimensions are changed (a = 4.94 Å; b = 9.09 Å; c = 20.64 Å) with a significant increase of c axis. Al atoms are in highly distorted sites with short Al–O bonding distances. These Al distorted sites drastically influence the Si tetrahedron positions which undergo various rotations. In general, the layered structural organization is maintained on a large scale. 1050 °C muscovite can be therefore, considered as an interesting high temperature substrate.

From X-rays (Fig. 1), PDF representations of muscovite–kaolinite composites at temperatures of 800, 1,000 and 1100 °C are plotted in Fig. 6. With the increase of temperature, some noticeable variations appear in curves.

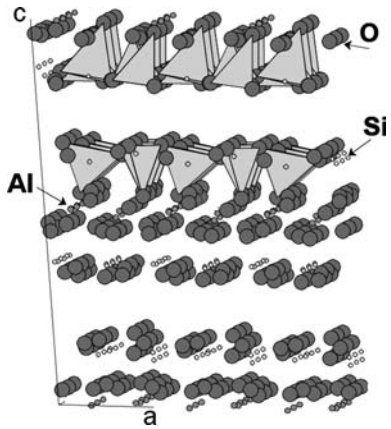

Fig. 5 Representation of the structural organization of muscovite at 1050 °C

The occurrence of Si–O bonds at 1.6 Å increases significantly and Al–O bonds in 6-fold environment at 1.9 Å increase above 850 °C. The behaviour of composite must be compared to the individual behaviour of each phyllosilicate. For kaolinite, Al atoms coordination changes from 6 to 4 or 5 at low temperature, but progressively becomes 6-fold above 900 °C [19, 20]. For muscovite, the Al environment also changes with temperature [10]. For our mixed material, both kaolinite and muscovite are transformed and it is therefore, not surprising that peak heights increase in the 1.6–1.9 Å range but also in the 3–3.5 Å range for the second neighbouring Al–O distances. At longer distances than single Si–O and Al–O bonds, peak amplitudes and positions at 3.05–3.25 Å, 4.1–4.45 Å, 5–5.15 Å and 7.2–7.6 Å also evolve significantly. These behaviours must be related to the short and long range structural organization of newly formed structures. Correspondingly, X-ray spectrums for muscovite–kaolinite at 1000 and 1100 °C (Fig. 1) present peaks from spinel, leucite and mainly mullite.

Discussion

For an ideal kaolinite, heated above 900 °C, either γ-alumina spinel or mullite recrystallize and the kinetics of this process depends on the kaolinite type and on thermal history [32]. For the used kaolinite, heated alone, this process is slow and only a small quantity of mullite appears below 1100 °C.

The PDF spectrum of composite materials heated at 800 °C has many similarities with other published experimental spectra from kaolinite alone, heated at 600 °C [20]. As the composite material contains also kaolinite, it can be supposed that PDF also shows typical information relative to that mineral. At this low temperature, no new phases are detectable on the curve and no specific interactions between minerals are supposed.

When the temperature increases up to 1000 and 1100 °C, PDF curve shapes change in both short range and long range

distances. It is obvious that the material structure reorganizes rapidly under the mutual interaction of metakaolinite and muscovite. X-ray curves of muscovite–kaolinite materials (Fig. 1) at 1000 and 1100 °C show large peaks from the newly formed spinel and mullite phase, but muscovite peaks disappear. At 1100 °C, mullite becomes the predominant phase, spinel quantity decreases sharply and muscovite is still detectable. The structural characteristics of mullite can be determined from peak positions in the 1100 °C pattern. Mullite lattice parameters are a = 7.550 Å, b = 7.682 Å and c = 2.884 Å. On the basis of Okada relation [33], mullite stoechiometry is $1.925SiO_2 3.075Al_2O_3$. These data are very close to those of 3:2 orthorhombic mullite (60 mol% of Al_2O_3). At a slightly lower temperature (1050 °C), mullite stoechiometry must change toward a higher alumina content, but the stoechiometry shift is supposed to be small. Correspondingly, the SEM photo of material at 1050 °C (Fig. 8) shows large and highly anisotropic crystals, which support the existence of orthorhombic mullite.

Correspondingly, the PDF curve of the 1100 °C material was simply approximated in Fig. 7 using 2 structures:—the high temperature muscovite (Fig. 5);—the 3:2 mullite phase ($Si_2Al_6O_{13}$, pbam).

Along with major phases, minor phases are also detected by X-ray diffraction (Fig. 1):—a potassium aluminium oxide ($KAl_{11}O_{17}$, P63/mmc, file N° 00-025-0617);—a leucite phase ($KAlSi_2O_6$). They preferentially crystallize under the increasing availability of K ions during heating, which was observed with the PDF simulation of the 1050 °C muscovite (Fig. 4). Peaks for K–Si distances at 3.78–3.81 Å and K–Al distances at 5.27–5.30 Å and 6.83–6.70 Å vanish (Fig. 3a) but for a successful fit we considered empty K sites. Correspondingly, K vacancy was reported [34] from 1100 °C muscovite. Authors considered that all K ions are lost during dehydroxylation. The available K ions contribute to the formation of a melted phase, mostly in combination with Si. Another study [35] reported that mostly Si in tetrahedrons, but also some Al, react with interlayer K ions to form a feldspar phase similar to leucite, without the separation of free silica (Fig. 1).

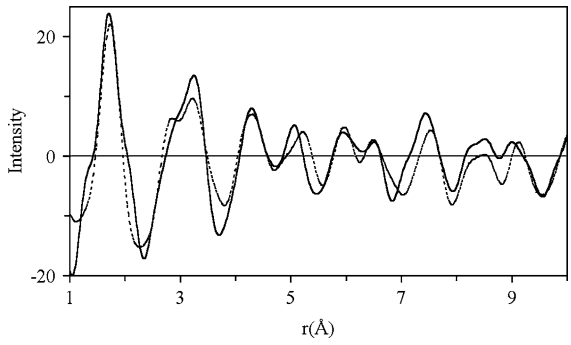

Fig. 7 Experimental (continuous line) and calculated PDF (dashed line) for muscovite–kaolinite material heated at 1100°C

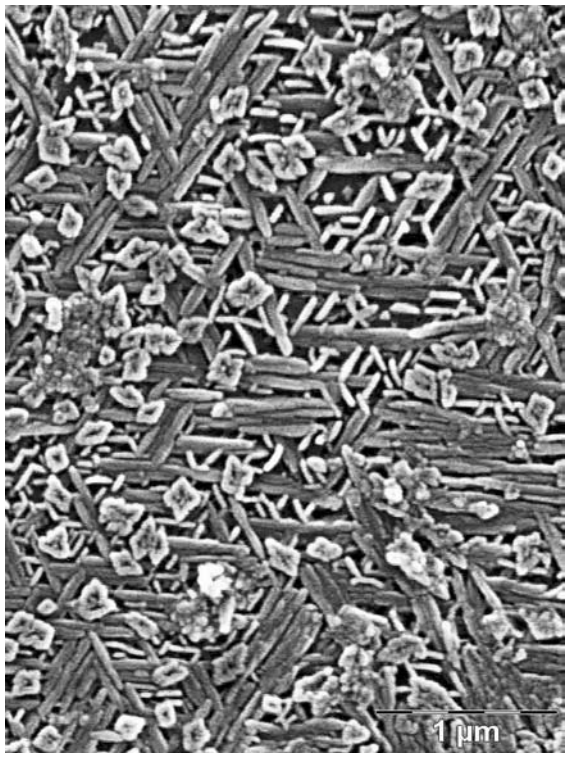

Fig. 8 SEM photo of mullite-kaolinite interface after heating at 1050 °C

In our composite material, the detected spinel-type phase has an hexagonal structure ($KAl_{11}O_{17}$, P63/mmc) [36]. Such an hexagonal phase was observed with heat-transformed kaolinite above 900 °C. It was shown that this phase originates from a topotactic transformation of metakaolinite and has similarities with γ-alumina.

In addition to the spinel-type phase, K ions must be involved in liquid formation in accordance with the ternary phase diagram SiO_2–Al_2O_3–K_2O [13]. The global composition of our material is in the primary field of mullite. The cooling path ends at the ternary eutectic, at 985 °C, but local deviations from that ideal line favour the existence of a first liquid at a temperature up to 1140 °C.

We suggest the presence of a very local melt at the muscovite–kaolinite interface in the 985–1140 °C temperature range. This point was assessed elsewhere with heterogeneous mixed minerals [34]. Our material presents a regular flat interface between muscovite and metakaolinite, which should favour the existence of an interfacial film above 985 °C. Although it is a transient melt because of the continuous enrichment by neighbouring Si and Al atoms, this liquid phase seems to act effectively during mullite formation.

SEM observation (Fig. 8) shows large mullite crystals at kaolinite–muscovite interfaces. An interesting behaviour is the occurrence of specific directions for mullite growth, with respect to the high temperature muscovite. All c axes

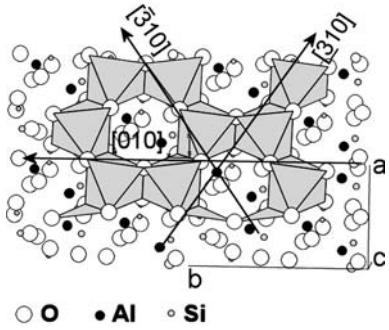

Fig. 9 Projection along (110) of the alumina sheet of Fig. 5

of mullite are parallel to $[001]_{musc}$ and an equivalent proportion of mullite *c* axes are parallel to either $[010]_{musc}$ or $[310]_{musc}$ and $[\bar{3}10]_{musc}$

This observation must be connected to the structure of dehydroxylated muscovite at 700 °C [10] and at 1050 °C (Fig. 5). A projection of the alumina sheet is given in Fig. 9, where alumina cells are connected along the above-mentioned directions. The alumina sheets of mica are disordered and subject to bond breaking, but the bonding stability is weaker for corner sharing polyhedrons than for edge sharing polyhedrons. Figure 9 illustrates that the preferential directions are maintained since further oxygen atoms are added for the reorganisation of new stable octahedrons. These octahedrons are partially bound to Si tetrahedrons along the $[010]_{musc}$ or $[310]_{musc}$ and $[\bar{3}10]_{musc}$. They form elementary chains for the nucleation of mullite and probably the subsequent formation of crystals. The mullite structure also shows chains of edge sharing octahedrons along the *c* axis, which are cross-linked by Si and Al tetrahedrons. Therefore, the $[001]_{mull}$ axis matches the $[010]_{musc}$ or $[310]_{musc}$ and $[\bar{3}10]_{musc}$ axes to form mullite. We propose that the nucleation process is highly favoured by the influence of a local melting on the mica surface where K ions react with metakaolinite sheets.

After the early formation of mullite crystals, a significant growth of mullite crystals also occurs. The coalescence of elementary chains is attained to form more stable structures (Fig. 8) with a larger size along the *c* axis (1–3 μm). The liquid, specifically localised at the interface, favours the achievement of a long-range order. This point is confirmed since higher temperature favours the growth of randomly oriented large crystals. Particularly, at 1140 °C, the ternary transition point for the global system is reached with a larger quantity of liquid phase.

Conclusion

Highly textured mullite was obtained at the muscovite–kaolinite interface, using large flakes of muscovite. Mullite nucleation and growth occurs at 1050 °C, epitaxially on the surface of the high temperature form of muscovite. This recrystallisation shows a clear topotactic character since main orientation relationships were found between mullite and muscovite. The $[001]_{mull}$ axis is oriented parallel to $[001]_{musc}$ and along $[010]_{musc}$ or $[310]_{musc}$ and $[\bar{3}10]_{musc}$ axes. In the 985–1140 °C temperature range, the recrystallisation is favoured by the presence of a liquid thin interlayer, which melt along the interface. Above 1140 °C, the quantity of liquid phase increases significantly and the muscovite dehydroxylation process is achieved, to give randomly oriented mullite.

References

1. Takenaka T, Sakata K (1980) Jpn J Appl Phys 19(1):31
2. Igarashi H, Matsunaga K, Taniai T, Okazaki K (1978) Am Ceram Soc Bull 57(9):815
3. Youngblood GE, Gordon RS (1978) Ceram Int 4(3):93
4. Hirao K, Ohashi M, Brito ME, Kanzaki S (1995) J Am Ceram Soc 78(6):1687
5. Seong-Hyong Hong, Messing GL (1999) J Am Ceram Soc 82(4):867
6. Kathryn L, Nagy L, Randall T, Cygan JM, Neil C (1999) Geochim Cosmochim Acta 63(16):2337
7. Wang ZJ, Bi HY, Kokawa H, Zhang L, Tsaur J, Ichiki M, Maeda R (2004) J Eur Ceram Soc 24(6):1629
8. Grim RE, Bradley WF, Brown G (1951) The mica clay minerals Brindley GW (ed) Mineralogical Society, London, 138
9. MacKenzie RC, Milne AA (1953) Mineral Mag 30:178
10. Guggenheim S, Chang YH, Koster van Groos AF (1987) Am Mineral 72:537
11. Udagawa S, Urabe K, Hasu H (1974) Jap Assoc Mineral Petrol Econ Geol 69:281
12. Mazzucato E, Artioli G, Gualtieri A (1999) Phys Chem Miner 26:375
13. Osborn EF, Muan A (1960) Phase Equilibrium Diagrams of Oxide Systems, The American Ceramic Society and the Edouard Orton Jr. Ceramic Foundation, Columbus, Ohio
14. Carty W, Senapati U (1998) J Am Ceram Soc 81(1):3
15. Bellotto M, Gualtieri A, Artioli G, Dark SM (1995) Phys Chem Miner 22:207
16. Bellotto M, Gualtieri A, Artioli G, Dark SM (1995) Phys Chem Miner 22:215
17. Drits VA, Tchoubar C (1990) X-ray diffraction by disordered lamellar structures, Springer-Verlag, Berlin, 233–303
18. Artioli G, Bellotto M, Gualtieri A, Pavese A (1995) Clays Clay Miner 4:438
19. Rocha J, Klinowski J (1990) Phys Chem Miner 17:179
20. Sanz J, Madani A, Serratosa JM, Moya JS, Aza S (1988) J Am Ceram Soc 71(10):C418
21. Gualtieri A, Bellotto M (1998) Phys Chem Miner 25:442
22. Klein HH, Stern WB, Weber W (1982) Schweizerische Mineralogische und Petrographische Mitteilungen 62(1):145
23. Pruett RJ, Webb HL (1993) Clays Clay Miner 41:514
24. Egami T, Billinge SJL (2003) Mater Today 6(6):57
25. Jeong IK, Thompson J, Proffen Th, Turner AMP, Billinge SJL (2001) J Appl Crystallogr 34(4):536
26. Proffen Th, Billinge SJL (1999) J Appl Crystallogr 32(3):572
27. Liang J, Hawthorne FC (1996) Can Mineral 34:115
28. Eberhart JP (1963) Bul Soc Fr Miner Cristallogr 86:213

29. Nicol AW (1964) Clays Clay Miner 12:11
30. Catti M, Ferraris G, Ivaldi G (1989) Eur J Mineral 1:625
31. Vassanyi I, Szabo A (1993) Mater Sci Forum 133–136:655
32. Castelein O, Soulestin B, Bonnet JP, Blanchart P (2001) Ceram Int 27(5):517
33. Ban T, Okada K (1992) J Am Soc 75(1):227
34. Rodriguez-Navarro C, Cultrone G, Sanchez-Navas A, Sebastian E (2003) Am Miner 88:713
35. Mackenzie KJD, Brown IWM, Cardile CM, Meinhold RH (1987) J Mat Sci 22:2645
36. Lee Sujeong, Kim Youn Joong, Moon Hi-Soo (1999) J Am Ceram Soc 82(10):2841